Hindawi Publishing Corporation
Mathematical Problems in Engineering
Volume 2014, Article ID 861708, 15 pages
http://dx.doi.org/10.1155/2014/861708

Research Article

Effects of Wall Shear Stress on MHD Conjugate Flow over an Inclined Plate in a Porous Medium with Ramped Wall Temperature

Arshad Khan,[1] Ilyas Khan,[2] Farhad Ali,[1] and Sharidan Shafie[1]

[1] *Department of Mathematical Sciences, Faculty of Science, Universiti Teknologi Malaysia, (UTM) 81310 Johor Bahru, Johor, Malaysia*
[2] *College of Engineering Majmaah University, P.O. Box 66, Majmaah 11952, Saudi Arabia*

Correspondence should be addressed to Sharidan Shafie; sharidan@utm.my

Received 3 December 2013; Accepted 22 February 2014; Published 2 April 2014

Academic Editor: Zhijun Zhang

This study investigates the effects of an arbitrary wall shear stress on unsteady magnetohydrodynamic (MHD) flow of a Newtonian fluid with conjugate effects of heat and mass transfer. The fluid is considered in a porous medium over an inclined plate with ramped temperature. The influence of thermal radiation in the energy equations is also considered. The coupled partial differential equations governing the flow are solved by using the Laplace transform technique. Exact solutions for velocity and temperature in case of both ramped and constant wall temperature as well as for concentration fields are obtained. It is found that velocity solutions are more general and can produce a huge number of exact solutions correlative to various fluid motions. Graphical results are provided for various embedded flow parameters and discussed in detail.

1. Introduction

The study of the natural convection heat transfer from different geometries of the surfaces has received much attention in recent years both analytically and experimentally. Amongst them a very little attention has been given to the problem of natural convection over an inclined plate as shown in Figure 1. Free convection heat transfer from an inclined surface has important role in making engineering devices and natural environment. Natural convection over an inclined plate was first studied experimentally by Rich [1]. A solution for the boundary layer on a horizontal plate showing that if the plate is heated and faces downwards or is cooled and faces upwards was presented by Stewartson [2]. Free convection heat transfer from an isothermal plate with arbitrary inclination was investigated by [3]. Chen et al. [4] have obtained a numerical solution for the problem of natural convection over an inclined plate with variable surface temperature. Ganesan and Ekambavanan [5] solved the unsteady natural convection boundary layer flow over a semi-infinite inclined plate with the wall temperature varying as the axial coordinate using an implicit finite difference scheme. The results of an experimental study on natural convection between inclined plates were presented by [6]. MHD natural convection from a nonisothermal inclined surface with multiple suction/injection slots embedded in a thermally stratified high porosity medium has been studied by [7]. A numerical solution of the transient free convection MHD flow of an incompressible viscous fluid past a semi-infinite inclined plate with variable surface heat and mass flux is presented by [8]. Unsteady free convection flow of water at its maximum density past a semi-infinite inclined plate with variable surface temperature of the plate was studied by [9]. An investigation deals with study of laminar natural convection flow of a viscous fluid over a semi-infinite flat plate inclined at a small angle to the horizontal with internal heat generation and variable viscosity was presented by [10]. Pressure effects on unsteady free convection and heat transfer flow of an incompressible fluid past a semi-infinite inclined plate with impulsive and uniformly accelerated motion were analyzed by [11]. Chemical reaction effects on MHD free convection flow through a porous medium bounded by

an inclined surface were studied by [12]. An analysis to study the heat and mass transfer characteristics of natural convection flow along horizontal and inclined plates with variable surface temperature/concentration or heat/mass flux under the combined buoyancy effects of thermal and mass diffusion was presented by [13]. A steady two dimensional MHD free convection and mass transfer flow past an inclined semi-infinite surface in the presence of heat generation has been studied numerically in [14]. A two-dimensional steady MHD mixed convection and mass transfer flow over a semi-infinite porous inclined plate in the presence of thermal radiation with variable suction and thermophoresis has been analyzed numerically by [15]. Heat and mass transfer of an incompressible viscous fluid past a semi-infinite inclined surface with first-order homogeneous chemical reaction by Lie group analysis had been presented by [16]. Recently, the exact analysis of combined effects of radiation and chemical reaction on the MHD free convection flow of an electrically conducting incompressible viscous fluid over an inclined plate embedded in a porous medium was studied by [17]. The inherent irreversibility and thermal stability in a gravity driven temperature dependent variable viscosity thin liquid film along an inclined heated plate with convective cooling were investigated by Makinde [18]. The inherent irreversibility in hydromagnetic boundary layer flow of variable viscosity fluid over a semi-infinite flat plate under the influence of thermal radiation and Newtonian heating was analyzed by [19]. Saha et al. [20] investigated that a natural convection boundary layer adjacent to an inclined semi-infinite plate subject to a temperature boundary condition which follows a ramped function up until some specified time and then remains constant. Saha et al. [21] also performed a scaling analysis for the transient boundary layer established adjacent to an inclined flat plate following a ramp cooling boundary condition. Recently, Ismail et al. [22] conducted the combined effects of heat and mass transfer on unsteady MHD free convection flow in a porous medium past an infinite inclined plate with ramped wall temperature. Fetecau et al. [23] investigated free convection flow near a vertical plate that applies arbitrary shear stress to the fluid when the thermal radiation and porosity effects are taken into consideration. However, from the literature, it is found that no study has been presented to investigate the unsteady MHD conjugate flow of an incompressible viscous fluid in a porous medium past over an inclined plate with ramped temperature in the presence of radiation under the boundary condition of wall shear stress.

Therefore, the aim of the present investigation is to provide exact solutions for MHD conjugate flow of a Newtonian fluid past an infinite plate that applies arbitrary shear stress to the fluid. More exactly, we consider the inclined plate situated in the (x, z) plane of a Cartesian coordinate system $Oxyz$, the domain of the flow is the porous half-space $y > 0$, and the arbitrary shear stress on the plate is given by $f(t)/\mu$, where $f(t)$ is an arbitrary function and μ is the viscosity. Closed form solutions of the initial and boundary value problems that govern the flow are obtained by means of the Laplace transform. Some special cases are extracted from the general solutions together with some limiting solutions in the literature. The results for velocity, temperature, and concentration profiles are plotted graphically and discussed for the embedded flow parameters.

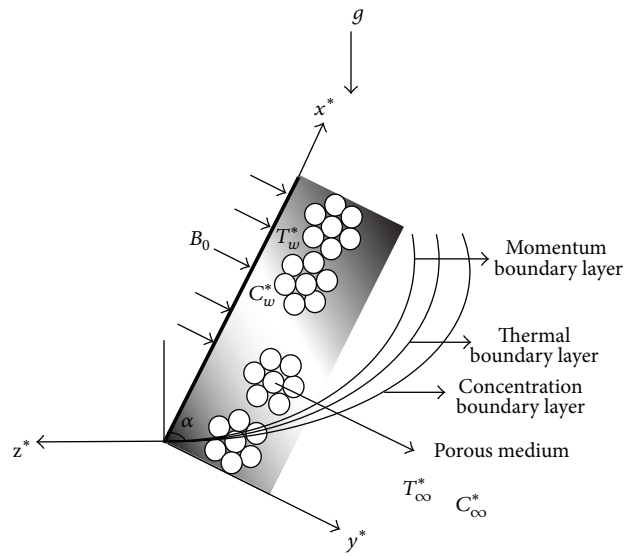

Figure 1: Physical configuration of the problem.

2. Mathematical Formulation

Let us consider the unsteady MHD free convection flow of an incompressible viscous fluid over an infinite inclined plate. The physical configuration of the problem is shown in Figure 1. The x-axis is taken along the plate and the y-axis is taken normal to it. Initially, both the plate and fluid are at stationary conditions with the constant temperature T_∞ and concentration C_∞. After time $t = 0^+$, the plate applies a time dependent shear stress $f(t)$ to the fluid along the x-axis. Meanwhile, the temperature of the plate is raised or lowered to $T_\infty + (T_w - T_\infty)(t/t_0)$ when $t \le t_0$, and, thereafter, for $t > t_0$, is maintained at constant temperature T_w and concentration is raised to C_w. The radiation term is also considered in the energy equation. However, the radiative heat flux is considered negligible in x-direction compared to y-direction. We assume that the flow is laminar and the fluid is grey absorbing-emitting radiation but no scattering medium. Using Boussinesq's approximation and neglecting the viscous dissipation, the equations governing the flow are given by [22]

$$\frac{\partial u}{\partial t} = \nu \frac{\partial^2 u}{\partial y^2} + g\beta_T (T - T_\infty)\cos(\alpha) + g\beta_C (C - C_\infty)\cos(\alpha) - \frac{\nu}{K}u - \frac{\sigma B_0^2}{\rho}u; \quad y, t > 0, \tag{1}$$

$$\rho C_p \frac{\partial T}{\partial t} = k\frac{\partial^2 T}{\partial y^2} - \frac{\partial q_r}{\partial y} \quad y, t > 0, \tag{2}$$

$$\frac{\partial C}{\partial t} = D\frac{\partial^2 C}{\partial y^2} \quad y, t > 0, \tag{3}$$

where u, T, C, ν, ρ, g, β_T, β_C, K, σ, B_0, C_p, k, q_r, and D are the velocity of the fluid in x-direction, its temperature and concentration, the kinematic viscosity, the constant density, the gravitational acceleration, the heat transfer coefficient, the mass transfer coefficient, the permeability of the porous medium, the electric conductivity of the fluid, the applied magnetic field, the heat capacity at constant pressure, the thermal conductivity, the radiative heat flux, and mass diffusivity.

The corresponding initial and boundary conditions are

$$\begin{aligned}
&u(y,0) = 0, \qquad T(y,0) = T_\infty,\\
&\qquad C(y,0) = C_\infty; \quad \forall y \geqslant 0,\\
&\frac{\partial u(0,t)}{\partial y} = \frac{f(t)}{\mu}, \quad C(0,t) = C_w; \quad t > 0,\\
&T(0,t) = T_\infty + (T_w - T_\infty)\frac{t}{t_0}, \quad 0 < t < t_0,\\
&T(0,t) = T_w; \quad t \geq t_0,\\
&u(\infty,t) = 0, \qquad T(\infty,t) = T_\infty,\\
&\qquad C(\infty,t) = C_\infty; \quad t > 0.
\end{aligned} \tag{4}$$

The radiation heat flux under Rosseland approximation for optically thick fluid [24–26] is given by

$$q_r = -\frac{4\sigma^*}{3k_R}\frac{\partial T^4}{\partial y}, \tag{5}$$

where σ^* and k_R is the Stefan-Boltzman constant and the mean absorption coefficient, respectively. We can see from (5) that the radiation term is nonlinear. Recently David Maxim Gururaj and Anjali Devi [27] used nonlinear radiation effects and studied MHD boundary layer flow with forced convection past a nonlinearly stretching surface with variable temperature. Therefore, we follow David Maxim Gururaj and Anjali Devi [27] and assume that the temperature differences within the flow are sufficiently small; that is, the difference between the fluid temperature and the free stream temperature is negligible, so that (5) can be linearized by expanding T into the Taylor series about T_∞, which after neglecting higher order terms takes the form

$$T^4 \approx 4T_\infty^3 T - 3T_\infty^4. \tag{6}$$

Substituting (6) into (5) and then putting the obtained result in (2), we get

$$\Pr\frac{\partial T}{\partial t} = \nu(1 + N_r)\frac{\partial^2 T}{\partial y^2}; \quad y, t > 0, \tag{7}$$

where Pr, ν, and N_r are defined by

$$\Pr = \frac{\mu C_p}{k}, \qquad \nu = \frac{\mu}{\rho}, \qquad N_r = \frac{16\sigma T_\infty^3}{3kk_R}. \tag{8}$$

By introducing the following dimensionless variables

$$\begin{aligned}
&u^* = u\sqrt{\frac{t_0}{\nu}}, \qquad T^* = \frac{T - T_\infty}{T_w - T_\infty},\\
&C^* = \frac{C - C_\infty}{C_w - C_\infty}, \qquad y^* = \frac{y}{\sqrt{\nu t_0}},\\
&t^* = \frac{t}{t_0}, \qquad f^*(t^*) = \frac{t_0}{\mu} f(t_0 t^*),
\end{aligned} \tag{9}$$

into (1), (3) and (7) and eleminating the star notations, we get

$$\frac{\partial u}{\partial t} = \frac{\partial^2 u}{\partial y^2} + \mathrm{Gr}T\cos\alpha + \mathrm{Gm}C\cos\alpha - K_p u - Mu, \tag{10}$$

$$\Pr_{\mathrm{eff}}\frac{\partial T}{\partial t} = \frac{\partial^2 T}{\partial y^2}, \tag{11}$$

$$\frac{\partial C}{\partial t} = \frac{1}{\mathrm{Sc}}\frac{\partial^2 C}{\partial y^2}, \tag{12}$$

where $\Pr_{\mathrm{eff}} = \Pr/(1 + N_r)$ is the effective Prandtl number [24, (10)] and

$$\begin{aligned}
&\mathrm{Gr} = \frac{g\beta_T(T_w - T_\infty)\nu}{U_0^3}, \qquad \mathrm{Gm} = \frac{g\beta_c(C_w - C_\infty)\nu}{U_0^3},\\
&M = \frac{\sigma B_0^2 t_0}{\rho}, \qquad \mathrm{Sc} = \frac{\nu}{D}, \qquad K_p = \frac{\nu t_0}{K}, \qquad t_0 = \frac{\nu}{U_0^2},
\end{aligned} \tag{13}$$

are the Grashof number, modified Grashof number, magnetic parameter, Schmidt number, the inverse permeability parameter for the porous medium, and the characteristic time, respectively.

The corresponding dimensionless initial and boundary conditions are

$$\begin{aligned}
&u(y,0) = 0, \quad T(y,0) = 0, \quad C(y,0) = 0; \quad \forall y \geq 0,\\
&\left.\frac{\partial u}{\partial y}\right|_{y=0} = f(t), \quad T(0,t) = t; \quad 0 < t \leq 1,\\
&T(0,t) = 1; \quad t > 1,\\
&C(0,t) = 1, \qquad C(\infty,t) = 0, \qquad T(\infty,t) = 0,\\
&u(\infty,t) = 0; \quad t > 0.
\end{aligned} \tag{14}$$

3. Solution of the Problem

In order to solve (10)–(12) under conditions (14), we use the Laplace transform technique and get the following differential equations:

$$q\bar{u}(y,q) = \frac{\partial^2 \bar{u}(y,q)}{\partial y^2} + \mathrm{Gr}\bar{T}(y,q)\cos(\alpha) + \mathrm{Gm}\bar{C}(y,q)\cos(\alpha) - K_p\bar{u}(y,q) - M\bar{u}(y,q), \tag{15}$$

$$\bar{T}(y,q) = \frac{1}{\mathrm{Pr}_{\mathrm{eff}}q}\frac{\partial^2 \bar{T}(y,q)}{\partial y^2}, \tag{16}$$

$$\bar{C}(y,q) = \frac{1}{\mathrm{Sc}q}\frac{\partial^2 \bar{C}(y,q)}{\partial y^2}, \tag{17}$$

with boundary conditions

$$\bar{C}(\infty,q) = 0, \quad \bar{C}(0,q) = \frac{1}{q}, \quad \bar{T}(\infty,q) = 0, \quad \bar{u}(\infty,q) = 0, \quad \left.\frac{\partial \bar{u}(y,q)}{\partial y}\right|_{y=0} = F(q), \quad T(0,q) = \frac{1-e^{-q}}{q^2}. \tag{18}$$

Solving (16) in view of (18), we get

$$\bar{T}(y,q) = \frac{1}{q^2}e^{-y\sqrt{q\mathrm{Pr}_{\mathrm{eff}}}} - \frac{e^{-q}}{q^2}e^{-y\sqrt{q\mathrm{Pr}_{\mathrm{eff}}}}, \tag{19}$$

which upon inverse Laplace transform gives

$$T(y,t) = f(y,t) - f(y,t-1)H(t-1), \tag{20}$$

where

$$f(y,t) = \left(\frac{\mathrm{Pr}_{\mathrm{eff}}y^2}{2} + t\right)\mathrm{erf}\,c\left(\frac{\sqrt{\mathrm{Pr}_{\mathrm{eff}}}y}{2\sqrt{t}}\right) - \sqrt{\frac{\mathrm{Pr}_{\mathrm{eff}}t}{\pi}}\,y\exp\left(\frac{-\mathrm{Pr}_{\mathrm{eff}}y^2}{4t}\right), \tag{21}$$

$$\left.\frac{\partial T(y,t)}{\partial y}\right|_{y=0} = \frac{2\sqrt{\mathrm{Pr}_{\mathrm{eff}}}}{\sqrt{\pi}}\left(\sqrt{t} - \sqrt{t-1}H(t-1)\right), \tag{22}$$

is the corresponding heat transfer rate also known as Nusselt number. Here $\mathrm{erf}(\cdot)$ and $\mathrm{erf}\,c(\cdot)$ denote the error function and complementary error function of Gauss.

Solution of (17) using boundary conditions from (18) yields

$$C(y,q) = \frac{1}{q}e^{-y\sqrt{\mathrm{Sc}q}}, \tag{23}$$

which upon inverse Laplace transform gives

$$C(y,t) = \mathrm{erf}\,c\left(\frac{y\sqrt{\mathrm{Sc}}}{2\sqrt{t}}\right), \tag{24}$$

$$\left.\frac{\partial C(y,t)}{\partial y}\right|_{y=0} = -\frac{\sqrt{\mathrm{Sc}}}{\sqrt{\pi t}}, \tag{25}$$

that is the corresponding mass transfer rate also known as Sherwood number.

The solution of (15) under boundary conditions (18) gives

$$\bar{u}(y,q) = \frac{a_1\sqrt{q}}{q^2(q-a_2)\sqrt{q+H_1}}e^{-y\sqrt{q+H_1}} - \frac{a_1\sqrt{q}e^{-q}}{q^2(q-a_2)\sqrt{q+H_1}}e^{-y\sqrt{q+H_1}} - \frac{F(q)}{\sqrt{q+H_1}}e^{-y\sqrt{q+H_1}} - \frac{a_3}{q^2(q-a_2)}e^{-y\sqrt{q\mathrm{Pr}_{\mathrm{eff}}}} + \frac{a_3e^{-q}}{q^2(q-a_2)}e^{-y\sqrt{q\mathrm{Pr}_{\mathrm{eff}}}} + \frac{a_4\sqrt{q}}{q(q-a_5)\sqrt{q+H_1}}e^{-y\sqrt{q+H_1}} - \frac{a_6}{q(q-a_5)}e^{-y\sqrt{q\mathrm{Sc}}}, \tag{26}$$

which upon inverse Laplace transform gives

$$u(y,t) = u_c(y,t) + u_m(y,t), \tag{27}$$

where

$$u_c(y,t) = a_1\int_0^t\left(\frac{e^{a_2(t-s)}\,\mathrm{erf}\left(\sqrt{a_2(t-s)}\right)}{(a_2)^{3/2}} - \frac{2\sqrt{t-s}}{\sqrt{\pi}a_2}\right)\times\frac{e^{-H_1s-y^2/4s}}{\sqrt{\pi s}}ds + \left[\frac{a_1}{a_2\pi}\int_0^{t-1}\frac{\left(2\sqrt{t-1-s}\right)e^{-H_1s-y^2/4s}}{\sqrt{s}}ds\right]\times H(t-1) - \left[\frac{a_1}{(a_2)^{3/2}\sqrt{\pi}}\int_0^{t-1}\left(\left(e^{a_2(t-1-s)-H_1s-y^2/4s}\,\mathrm{erf}\times\left(\sqrt{a_2(t-1-s)}\right)\right)\times(\sqrt{s})^{-1}\right)ds\right]$$

$$\times H(t-1)$$
$$+a_4\int_0^t\left(\frac{e^{a_5(t-s)}\operatorname{erf}\left(\sqrt{a_5(t-s)}\right)}{\sqrt{a_5}}-\frac{2\sqrt{t-s}}{\sqrt{\pi}a_2}\right)\times\frac{e^{-H_1 s-y^2/4s}}{\sqrt{\pi s}}ds$$
$$+\frac{a_3}{a_2}\left(t+\frac{\mathrm{Pr}_{\mathrm{eff}}y^2}{2}\right)\operatorname{erf}c\left(\frac{y\sqrt{\mathrm{Pr}_{\mathrm{eff}}}}{2\sqrt{t}}\right)$$
$$-\frac{a_3}{a_2}\frac{y\sqrt{\mathrm{Pr}_{\mathrm{eff}}}\sqrt{t}}{\sqrt{\pi}}e^{-y^2\mathrm{Pr}_{\mathrm{eff}}/4t}+\frac{a_3}{a_2^2}\operatorname{erf}c\left(\frac{y\sqrt{\mathrm{Pr}_{\mathrm{eff}}}}{2\sqrt{t}}\right)$$
$$-\frac{a_3e^{a_2t+y\sqrt{\mathrm{Pr}_{\mathrm{eff}}a_2}}}{2a_2^2}\operatorname{erf}c\left(\frac{y\sqrt{\mathrm{Pr}_{\mathrm{eff}}}}{2\sqrt{t}}+\sqrt{a_2t}\right)$$
$$-\frac{a_3e^{a_2t-y\sqrt{\mathrm{Pr}_{\mathrm{eff}}a_2}}}{2a_2^2}\operatorname{erf}c\left(\frac{y\sqrt{\mathrm{Pr}_{\mathrm{eff}}}}{2\sqrt{t}}-\sqrt{a_2t}\right)$$
$$-\frac{a_3}{a_2}\left((t-1)+\frac{\mathrm{Pr}_{\mathrm{eff}}y^2}{2}\right)\operatorname{erf}c\left(\frac{y\sqrt{\mathrm{Pr}_{\mathrm{eff}}}}{2\sqrt{t-1}}\right)H(t-1)$$
$$+\frac{a_3}{a_2}\frac{y\sqrt{\mathrm{Pr}_{\mathrm{eff}}}\sqrt{t-1}}{\sqrt{\pi}}e^{-y^2\mathrm{Pr}_{\mathrm{eff}}/4(t-1)}H(t-1)$$
$$-\frac{a_3}{a_2^2}\operatorname{erf}c\left(\frac{y\sqrt{\mathrm{Pr}_{\mathrm{eff}}}}{2\sqrt{t-1}}\right)H(t-1)+\frac{a_6}{a_5}\operatorname{erf}c\left(\frac{y\sqrt{\mathrm{Sc}}}{2\sqrt{t}}\right)$$
$$+\frac{a_3e^{a_2(t-1)+y\sqrt{\mathrm{Pr}_{\mathrm{eff}}a_2}}}{2a_2^2}\operatorname{erf}c\left(\frac{y\sqrt{\mathrm{Pr}_{\mathrm{eff}}}}{2\sqrt{t-1}}+\sqrt{a_2(t-1)}\right)\times H(t-1)$$
$$+\frac{a_3e^{a_2(t-1)-y\sqrt{\mathrm{Pr}_{\mathrm{eff}}a_2}}}{2a_2^2}\operatorname{erf}c\left(\frac{y\sqrt{\mathrm{Pr}_{\mathrm{eff}}}}{2\sqrt{t-1}}-\sqrt{a_2(t-1)}\right)\times H(t-1)$$
$$-\frac{a_6e^{a_5t-y\sqrt{a_5\mathrm{Sc}}}}{2a_5}\operatorname{erf}c\left(\frac{y\sqrt{\mathrm{Sc}}}{2\sqrt{t}}-\sqrt{a_5t}\right)$$
$$-\frac{a_6e^{a_5t+y\sqrt{a_5\mathrm{Sc}}}}{2a_5}\operatorname{erf}c\left(\frac{y\sqrt{\mathrm{Sc}}}{2\sqrt{t}}+\sqrt{a_5t}\right),\tag{28}$$

$$u_m(y,t)=-\frac{1}{\sqrt{\pi}}\int_0^t\frac{f(t-s)\,e^{-H_1s-y^2/4s}}{\sqrt{s}},\tag{29}$$

correspond to the convective and mechanical parts of velocity.

It is noted from (20) and (28) that $T(y,t)$ is valid for all positive values of $\mathrm{Pr}_{\mathrm{eff}}$ while the $u_c(y,t)$ is not valid for $\mathrm{Pr}_{\mathrm{eff}}=1$. Therefore, to get $u_c(y,t)$ when the effective Prandtl number is not equal to one, we make $\mathrm{Pr}_{\mathrm{eff}}=1$ into (11), use a similar procedure as discussed above, and obtain

$$\bar{u}(y,q)=\frac{-a_{14}}{q^{3/2}\sqrt{q+H_1}}e^{-y\sqrt{q+H_1}}+\frac{a_{14}e^{-q}}{q^{3/2}\sqrt{q+H_1}}e^{-y\sqrt{q+H_1}}-\frac{F(q)}{\sqrt{q+H_1}}e^{-y\sqrt{q+H_1}}+\frac{a_{14}}{q^2}e^{-y\sqrt{q}}-\frac{a_{14}e^{-q}}{q^2}e^{-y\sqrt{q}}+\frac{a_4\sqrt{q}}{q(q-a_5)\sqrt{q+H_1}}e^{-y\sqrt{q+H_1}}-\frac{a_6}{q(q-a_5)}e^{-y\sqrt{q\mathrm{Sc}}}.\tag{30}$$

By taking inverse Laplace transform, we find that

$$u(y,t)=-\frac{2a_{14}}{\pi}\int_0^t\frac{\sqrt{t-s}e^{-H_1s-y^2/4s}}{\sqrt{s}}ds+\left(\frac{2a_{14}}{\pi}\int_0^{t-1}\frac{\sqrt{t-1-s}e^{-H_1s-y^2/4s}}{\sqrt{s}}ds\right)H(t-1)$$
$$+a_4\int_0^t\left(\frac{e^{a_5(t-s)}\operatorname{erf}\left(\sqrt{a_5(t-s)}\right)}{\sqrt{a_5}}-\frac{2\sqrt{t-s}}{\sqrt{\pi}a_2}\right)\times\frac{e^{-H_1s-y^2/4s}}{\sqrt{\pi s}}ds$$
$$+a_{14}\left[\left(t+\frac{y^2}{2}\right)\operatorname{erf}c\left(\frac{y}{2\sqrt{t}}\right)-\frac{y\sqrt{t}}{\sqrt{\pi}}e^{-y^2/4t}\right]-\frac{a_6e^{a_5t-y\sqrt{a_5\mathrm{Sc}}}}{2a_5}\operatorname{erf}c\left(\frac{y\sqrt{\mathrm{Sc}}}{2\sqrt{t}}-\sqrt{a_5t}\right)$$
$$-a_{14}\left[\left(t-1+\frac{y^2}{2}\right)\operatorname{erf}c\left(\frac{y}{2\sqrt{t-1}}\right)-\frac{y\sqrt{t-1}}{\sqrt{\pi}}e^{-y^2/4(t-1)}\right]H(t-1)$$
$$+\frac{a_6}{a_5}\operatorname{erf}c\left(\frac{y\sqrt{\mathrm{Sc}}}{2\sqrt{t}}\right)-\frac{1}{\sqrt{\pi}}\int_0^t\frac{f(t-s)\,e^{-H_1s-y^2/4s}}{\sqrt{s}}ds-\frac{a_6e^{a_5t+y\sqrt{a_5\mathrm{Sc}}}}{2a_5}\operatorname{erf}c\left(\frac{y\sqrt{\mathrm{Sc}}}{2\sqrt{t}}+\sqrt{a_5t}\right),\tag{31}$$

where

$$a_1=\frac{\cos\alpha\mathrm{Gr}\sqrt{\mathrm{Pr}_{\mathrm{eff}}}}{\mathrm{Pr}_{\mathrm{eff}}-1},\quad a_2=\frac{H_1}{\mathrm{Pr}_{\mathrm{eff}}-1},\quad a_3=\frac{\mathrm{Gr}\cos\alpha}{\mathrm{Pr}_{\mathrm{eff}}-1},$$
$$a_4=\frac{\cos\alpha\mathrm{Gm}\sqrt{\mathrm{Sc}}}{\mathrm{Sc}-1},\quad a_5=\frac{H_1}{\mathrm{Sc}-1},\quad a_6=\frac{\cos\alpha\mathrm{Gm}}{\mathrm{Sc}-1},$$

$$a_7 = \frac{\cos\alpha \mathrm{Gr}\sqrt{\mathrm{Pr}}}{\mathrm{Pr}-1}, \quad a_8 = \frac{H_1}{\mathrm{Pr}-1}, \quad a_9 = \frac{\cos\alpha \mathrm{Gr}}{\mathrm{Pr}-1},$$
$$a_{10} = \frac{K_p}{\mathrm{Pr}_{\mathrm{eff}}-1}, \quad a_{11} = \frac{K_p}{\mathrm{Sc}-1}, \quad a_{12} = \frac{M}{\mathrm{Pr}_{\mathrm{eff}}-1},$$
$$a_{13} = \frac{M}{\mathrm{Sc}-1}, \quad a_{14} = \frac{\cos\alpha \mathrm{Gr}}{H_1}, \quad H_1 = K_p + M. \tag{32}$$

4. Plate with Constant Temperature

Equations (20) and (27) give analytical expressions for the temperature and velocity near an inclined plate with ramped temperature. In order to highlight the effect of the ramped temperature distribution of the boundary on the flow, it is important to compare such a flow with the one near a plate with constant temperature. It can be shown that the temperature, rate of heat transfer, and velocity for the flow near an isothermal plate are

$$T(y,t) = \mathrm{erfc}\left(\frac{y\sqrt{\mathrm{Pr}_{\mathrm{eff}}}}{2\sqrt{t}}\right), \tag{33}$$

$$\frac{\partial T(0,t)}{\partial y} = -\frac{\sqrt{\mathrm{Pr}_{\mathrm{eff}}}}{\sqrt{\pi t}}, \tag{34}$$

$$\begin{aligned} u_c(y,t) &= \frac{a_1}{\sqrt{\pi a_2}}\int_0^t \frac{e^{a_2(t-s)-H_1 s-y^2/4s}\,\mathrm{erfc}\left(\sqrt{a_2(t-s)}\right)}{\sqrt{s}}ds \\ &+ \frac{a_4}{\sqrt{\pi a_5}}\int_0^t \frac{e^{a_5(t-s)-H_1 s-y^2/4s}\,\mathrm{erfc}\left(\sqrt{a_5(t-s)}\right)}{\sqrt{s}}ds \\ &- \frac{a_3}{2a_2}e^{a_2 t+y\sqrt{a_2\mathrm{Pr}_{\mathrm{eff}}}}\,\mathrm{erfc}\left(\frac{y\sqrt{\mathrm{Pr}_{\mathrm{eff}}}}{2\sqrt{t}}+\sqrt{a_2 t}\right) \\ &- \frac{a_3}{2a_2}e^{a_2 t-y\sqrt{a_2\mathrm{Pr}_{\mathrm{eff}}}}\,\mathrm{erfc}\left(\frac{y\sqrt{\mathrm{Pr}_{\mathrm{eff}}}}{2\sqrt{t}}-\sqrt{a_2 t}\right) \\ &- \frac{a_6}{2a_5}e^{a_5 t-y\sqrt{a_5\mathrm{Sc}}}\,\mathrm{erfc}\left(\frac{y\sqrt{\mathrm{Sc}}}{2\sqrt{t}}-\sqrt{a_5 t}\right) \\ &+ \frac{a_3}{a_2}\,\mathrm{erfc}\left(\frac{y\sqrt{\mathrm{Pr}_{\mathrm{eff}}}}{2\sqrt{t}}\right) + \frac{a_6}{a_5}\,\mathrm{erfc}\left(\frac{y\sqrt{\mathrm{Sc}}}{2\sqrt{t}}\right) \\ &- \frac{a_6}{2a_5}e^{a_5 t+y\sqrt{a_5\mathrm{Sc}}}\,\mathrm{erfc}\left(\frac{y\sqrt{\mathrm{Sc}}}{2\sqrt{t}}+\sqrt{a_5 t}\right), \end{aligned} \tag{35}$$

$$u_m(y,t) = -\frac{1}{\sqrt{\pi}}\int_0^t \frac{f(t-s)\,e^{-H_1 s-y^2/4s}}{\sqrt{s}}ds. \tag{36}$$

As previously, (36) is not valid for $\mathrm{Pr}_{\mathrm{eff}} = 1$. Therefore we calculate separately solution for velocity by taking $\mathrm{Pr}_{\mathrm{eff}} = 1$ into (11) and finally get

$$\begin{aligned} u(y,t) &= a_{14}\,\mathrm{erfc}\left(\frac{y}{2\sqrt{t}}\right) - \frac{a_{14}}{\sqrt{\pi}}\int_0^t \frac{e^{-H_1 s-y^2/4s}}{\sqrt{(t-s)\,s}}ds \\ &+ \frac{a_4}{\sqrt{\pi a_5}}\int_0^t \frac{e^{a_5(t-s)-H_1 s-y^2/4s}\,\mathrm{erf}\left(\sqrt{a_5(t-s)}\right)}{\sqrt{s}}ds \\ &+ \frac{a_6}{a_5}\,\mathrm{erfc}\left(\frac{y\sqrt{\mathrm{Sc}}}{2\sqrt{t}}\right) - \frac{1}{\sqrt{\pi}}\int_0^t \frac{f(t-s)\,e^{-H_1 s-y^2/4s}}{\sqrt{s}}ds \\ &- \frac{a_6}{2a_5}e^{a_5 t+y\sqrt{a_5\mathrm{Sc}}}\,\mathrm{erfc}\left(\frac{y\sqrt{\mathrm{Sc}}}{2\sqrt{t}}+\sqrt{a_5 t}\right) \\ &- \frac{a_6}{2a_5}e^{a_5 t-y\sqrt{a_5\mathrm{Sc}}}\,\mathrm{erfc}\left(\frac{y\sqrt{\mathrm{Sc}}}{2\sqrt{t}}-\sqrt{a_5 t}\right). \end{aligned} \tag{37}$$

5. Limiting Cases

In this section, we discuss few limiting cases of our general solutions.

5.1. Solution in the Absence of Porous Effects for Ramped and Constant Wall Temperature ($K_p \to 0$). Consider

$$\begin{aligned} u(y,t) &= a_1\int_0^t \left(\frac{e^{a_{12}(t-s)}\,\mathrm{erfc}\left(\sqrt{a_{12}(t-s)}\right)}{(a_{12})^{3/2}} - \frac{2\sqrt{t-s}}{\sqrt{\pi}a_{12}}\right) \\ &\quad \times \frac{e^{-Ms-y^2/4s}}{\sqrt{\pi s}}ds \\ &+ \left[\frac{a_1}{a_{12}\pi}\int_0^{t-1}\frac{\left(2\sqrt{t-1-s}\right)e^{-Ms-y^2/4s}}{\sqrt{s}}ds\right]H(t-1) \\ &- \left[\frac{a_1}{(a_{12})^{3/2}\sqrt{\pi}}\int_0^{t-1}\left(\left(e^{a_{12}(t-1-s)-Ms-y^2/4s}\,\mathrm{erf}\right.\right.\right. \\ &\quad \left.\left.\left.\times\left(\sqrt{a_{12}(t-1-s)}\right)\right)\times\left(\sqrt{s}\right)^{-1}\right)ds\right] \\ &\times H(t-1) \\ &+ a_4\int_0^t\left(\frac{e^{a_{13}(t-s)}\,\mathrm{erf}\left(\sqrt{a_{13}(t-s)}\right)}{\sqrt{a_{13}}} - \frac{2\sqrt{t-s}}{\sqrt{\pi}a_{12}}\right) \\ &\quad \times \frac{e^{-Ms-y^2/4s}}{\sqrt{\pi s}}ds \end{aligned}$$

$$+\frac{a_3}{a_{12}}\left(t+\frac{\mathrm{Pr}_{\mathrm{eff}}y^2}{2}\right)\mathrm{erf}\,c\left(\frac{y\sqrt{\mathrm{Pr}_{\mathrm{eff}}}}{2\sqrt{t}}\right)$$
$$-\frac{1}{\sqrt{\pi}}\int_0^t\frac{f(t-s)\,e^{-Ms-y^2/4s}}{\sqrt{s}}ds$$
$$-\frac{a_3}{a_{12}}\frac{y\sqrt{\mathrm{Pr}_{\mathrm{eff}}}\sqrt{t}}{\sqrt{\pi}}e^{-y^2\mathrm{Pr}_{\mathrm{eff}}/4t}+\frac{a_3}{a_{12}^2}\mathrm{erf}\,c\left(\frac{y\sqrt{\mathrm{Pr}_{\mathrm{eff}}}}{2\sqrt{t}}\right)$$
$$-\frac{a_3e^{a_{12}t+y\sqrt{\mathrm{Pr}_{\mathrm{eff}}a_{12}}}}{2a_{12}^2}\mathrm{erf}\,c\left(\frac{y\sqrt{\mathrm{Pr}_{\mathrm{eff}}}}{2\sqrt{t}}+\sqrt{a_{12}t}\right)$$
$$-\frac{a_3e^{a_{12}t-y\sqrt{\mathrm{Pr}_{\mathrm{eff}}a_{12}}}}{2a_{12}^2}\mathrm{erf}\,c\left(\frac{y\sqrt{\mathrm{Pr}_{\mathrm{eff}}}}{2\sqrt{t}}-\sqrt{a_{12}t}\right)$$
$$-\frac{a_3}{a_{12}}\left((t-1)+\frac{\mathrm{Pr}_{\mathrm{eff}}y^2}{2}\right)\mathrm{erf}\,c\left(\frac{y\sqrt{\mathrm{Pr}_{\mathrm{eff}}}}{2\sqrt{t-1}}\right)H(t-1)$$
$$+\frac{a_3}{a_{12}}\frac{y\sqrt{\mathrm{Pr}_{\mathrm{eff}}}\sqrt{t-1}}{\sqrt{\pi}}e^{-y^2\mathrm{Pr}_{\mathrm{eff}}/4(t-1)}H(t-1)$$
$$-\frac{a_6e^{a_{13}t-y\sqrt{a_{13}\mathrm{Sc}}}}{2a_{13}}\mathrm{erf}\,c\left(\frac{y\sqrt{\mathrm{Sc}}}{2\sqrt{t}}-\sqrt{a_{13}t}\right)$$
$$-\frac{a_3}{a_{12}^2}\mathrm{erf}\,c\left(\frac{y\sqrt{\mathrm{Pr}_{\mathrm{eff}}}}{2\sqrt{t-1}}\right)H(t-1)+\frac{a_6}{a_{13}}\mathrm{erf}\,c\left(\frac{y\sqrt{\mathrm{Sc}}}{2\sqrt{t}}\right)$$
$$+\frac{a_3e^{a_{12}(t-1)+y\sqrt{\mathrm{Pr}_{\mathrm{eff}}a_{12}}}}{2a_{12}^2}\mathrm{erf}\,c\left(\frac{y\sqrt{\mathrm{Pr}_{\mathrm{eff}}}}{2\sqrt{t-1}}+\sqrt{a_{12}(t-1)}\right)$$
$$\times H(t-1)$$
$$+\frac{a_3e^{a_{12}(t-1)-y\sqrt{\mathrm{Pr}_{\mathrm{eff}}a_{12}}}}{2a_{12}^2}\mathrm{erf}\,c\left(\frac{y\sqrt{\mathrm{Pr}_{\mathrm{eff}}}}{2\sqrt{t-1}}-\sqrt{a_{12}(t-1)}\right)$$
$$\times H(t-1)$$
$$-\frac{a_6e^{a_{13}t+y\sqrt{a_{13}\mathrm{Sc}}}}{2a_{13}}\mathrm{erf}\,c\left(\frac{y\sqrt{\mathrm{Sc}}}{2\sqrt{t}}+\sqrt{a_{13}t}\right),$$

$$u(y,t)$$
$$=\frac{a_1}{\sqrt{\pi a_{12}}}\int_0^t\frac{e^{a_{12}(t-s)-Ms-y^2/4s}\,\mathrm{erf}\left(\sqrt{a_{12}(t-s)}\right)}{\sqrt{s}}ds$$
$$+\frac{a_4}{\sqrt{\pi a_{13}}}\int_0^t\frac{e^{a_{13}(t-s)-Ms-y^2/4s}\,\mathrm{erf}\left(\sqrt{a_{13}(t-s)}\right)}{\sqrt{s}}ds$$
$$-\frac{a_6}{2a_{13}}e^{a_{13}t-y\sqrt{a_{13}\mathrm{Sc}}}\mathrm{erf}\,c\left(\frac{y\sqrt{\mathrm{Sc}}}{2\sqrt{t}}-\sqrt{a_{13}t}\right)$$
$$-\frac{a_3}{2a_{12}}e^{a_{12}t+y\sqrt{a_{12}\mathrm{Pr}_{\mathrm{eff}}}}\mathrm{erf}\,c\left(\frac{y\sqrt{\mathrm{Pr}_{\mathrm{eff}}}}{2\sqrt{t}}+\sqrt{a_{12}t}\right)$$
$$-\frac{a_3}{2a_{12}}e^{a_{12}t-y\sqrt{a_{12}\mathrm{Pr}_{\mathrm{eff}}}}\mathrm{erf}\,c\left(\frac{y\sqrt{\mathrm{Pr}_{\mathrm{eff}}}}{2\sqrt{t}}-\sqrt{a_{12}t}\right)$$
$$+\frac{a_3}{a_{12}}\mathrm{erf}\,c\left(\frac{y\sqrt{\mathrm{Pr}_{\mathrm{eff}}}}{2\sqrt{t}}\right)+\frac{a_6}{a_{13}}\mathrm{erf}\,c\left(\frac{y\sqrt{\mathrm{Sc}}}{2\sqrt{t}}\right)$$
$$-\frac{a_6}{2a_{13}}e^{a_{13}t+y\sqrt{a_{13}\mathrm{Sc}}}\mathrm{erf}\,c\left(\frac{y\sqrt{\mathrm{Sc}}}{2\sqrt{t}}+\sqrt{a_{13}t}\right).$$
(38)

5.2. Solution in the Absence of Thermal Radiation ($N_r \to 0$). In the absence of thermal radiation, the corresponding solutions for ramped and constant wall temperature are directly obtained from the general solutions (20), (22), (27), and (33)–(36) by taking $N_r \to 0$ and replacing $\mathrm{Pr}_{\mathrm{eff}}$ by Pr; that is,

$$u(y,t)$$
$$=a_7\int_0^t\left(\frac{e^{a_8(t-s)}\,\mathrm{erf}\left(\sqrt{a_8(t-s)}\right)}{(a_8)^{3/2}}-\frac{2\sqrt{t-s}}{\sqrt{\pi}a_8}\right)$$
$$\times\frac{e^{-H_1s-y^2/4s}}{\sqrt{\pi s}}ds$$
$$+\left[\frac{a_7}{\pi a_8}\int_0^{t-1}\frac{2\sqrt{t-1-s}e^{-H_1s-y^2/4s}}{\sqrt{s}}ds\right]$$
$$\times H(t-1)$$
$$-\left[\frac{a_7}{(a_8)^{3/2}\sqrt{\pi}}\int_0^{t-1}\left(\left(\mathrm{erf}\left(\sqrt{a_8(t-1-s)}\right)\right.\right.\right.$$
$$\left.\left.\left.\times e^{a_8(t-1-s)-H_1s-y^2/4s}\right)\right.$$
$$\left.\times\left(\sqrt{s}\right)^{-1}\right)ds\Bigg]$$
$$\times H(t-1s)$$
$$+a_4\int_0^t\left(\frac{e^{a_5(t-s)}\,\mathrm{erf}\left(\sqrt{a_5(t-s)}\right)}{\sqrt{a_5}}-\frac{2\sqrt{t-s}}{\sqrt{\pi}a_8}\right)$$
$$\times\frac{e^{-H_1s-y^2/4s}}{\sqrt{\pi s}}ds$$
$$+\frac{a_9}{a_8}\left(t+\frac{\mathrm{Pr}y^2}{2}\right)\mathrm{erf}\,c\left(\frac{y\sqrt{\mathrm{Pr}}}{2\sqrt{t}}\right)$$
$$-\frac{1}{\sqrt{\pi}}\int_0^t\frac{f(t-s)\,e^{-H_1s-y^2/4s}}{\sqrt{s}}ds$$
$$-\frac{a_9}{a_8}\frac{y\sqrt{\mathrm{Pr}}\sqrt{t}}{\sqrt{\pi}}e^{-y^2\mathrm{Pr}/4t}+\frac{a_9}{a_8^2}\mathrm{erf}\,c\left(\frac{y\sqrt{\mathrm{Pr}}}{2\sqrt{t}}\right)$$
$$-\frac{a_9e^{a_8t+y\sqrt{\mathrm{Pr}a_8}}}{2a_8^2}\mathrm{erf}\,c\left(\frac{y\sqrt{\mathrm{Pr}}}{2\sqrt{t}}+\sqrt{a_8t}\right)$$

$$
\begin{aligned}
&- \frac{a_9 e^{a_8 t - y\sqrt{\Pr a_8}}}{2a_8^2} \operatorname{erf} c\left(\frac{y\sqrt{\Pr}}{2\sqrt{t}} - \sqrt{a_8 t}\right) \\
&- \frac{a_9}{a_8}\left((t-1) + \frac{\Pr y^2}{2}\right) \operatorname{erf} c\left(\frac{y\sqrt{\Pr}}{2\sqrt{t-1}}\right) H(t-1) \\
&- \frac{a_9}{a_8} \operatorname{erf} c\left(\frac{y\sqrt{\Pr}}{2\sqrt{t-1}}\right) H(t-1) \\
&+ \frac{a_9}{a_8} \frac{y\sqrt{\Pr}\sqrt{t-1}}{\sqrt{\pi}} e^{-y^2 \Pr/4(t-1)} H(t-1) \\
&+ \frac{a_9 e^{a_8(t-1) + y\sqrt{\Pr a_8}}}{2a_8^2} \operatorname{erf} c\left(\frac{y\sqrt{\Pr}}{2\sqrt{t-1}} + \sqrt{a_8(t-1)}\right) \\
&\times H(t-1) \\
&+ \frac{a_9 e^{a_{12}(t-1) - y\sqrt{\Pr a_{12}}}}{2a_8^2} \operatorname{erf} c\left(\frac{y\sqrt{\Pr}}{2\sqrt{t-1}} - \sqrt{a_8(t-1)}\right) \\
&\times H(t-1) \\
&- \frac{a_6 e^{a_5 t + y\sqrt{a_5 \mathrm{Sc}}}}{2a_5} \operatorname{erf} c\left(\frac{y\sqrt{\mathrm{Sc}}}{2\sqrt{t}} + \sqrt{a_5 t}\right) \\
&+ \frac{a_6}{a_5} \operatorname{erf} c\left(\frac{y\sqrt{\mathrm{Sc}}}{2\sqrt{t}}\right) \\
&- \frac{a_6 e^{a_5 t - y\sqrt{a_5 \mathrm{Sc}}}}{2a_5} \operatorname{erf} c\left(\frac{y\sqrt{\mathrm{Sc}}}{2\sqrt{t}} - \sqrt{a_5 t}\right), \\
T(y,t) &= f_1(y,t) - f_1(y,t-1) H(t-1),
\end{aligned}
\tag{39}
$$

where

$$
\begin{aligned}
f_1(y,t) &= \left(\frac{\Pr y^2}{2} + t\right) \operatorname{erf} c\left(\frac{\sqrt{\Pr} y}{2\sqrt{t}}\right) \\
&\quad - \sqrt{\frac{\Pr t}{\pi}}\, y \exp\left(\frac{-\Pr y^2}{4t}\right), \\
\left.\frac{\partial T(y,t)}{\partial y}\right|_{y=0} &= \frac{2\sqrt{\Pr}}{\sqrt{\pi}}\left(\sqrt{t} - \sqrt{t-1} H(t-1)\right), \\
u(y,t) &= \frac{a_7}{\sqrt{\pi a_8}} \int_0^t \frac{e^{a_8(t-s) - H_1 s - y^2/4s} \operatorname{erf}\left(\sqrt{a_8(t-s)}\right)}{\sqrt{s}} ds \\
&\quad + \frac{a_4}{\sqrt{\pi a_5}} \int_0^t \frac{e^{a_5(t-s) - H_1 s - y^2/4s} \operatorname{erf}\left(\sqrt{a_5(t-s)}\right)}{\sqrt{s}} ds \\
&\quad - \frac{a_9}{2a_8} e^{a_8 t + y\sqrt{a_8 \Pr}} \operatorname{erf} c\left(\frac{y\sqrt{\Pr}}{2\sqrt{t}} + \sqrt{a_8 t}\right) \\
&\quad - \frac{a_9}{2a_8} e^{a_8 t - y\sqrt{a_8 \Pr}} \operatorname{erf} c\left(\frac{y\sqrt{\Pr}}{2\sqrt{t}} - \sqrt{a_8 t}\right) \\
&\quad + \frac{a_9}{a_8} \operatorname{erf} c\left(\frac{y\sqrt{\Pr}}{2\sqrt{t}}\right) + \frac{a_6}{a_5} \operatorname{erf} c\left(\frac{y\sqrt{\mathrm{Sc}}}{2\sqrt{t}}\right) \\
&\quad - \frac{a_6}{2a_5} e^{a_5 t + y\sqrt{a_5 \mathrm{Sc}}} \operatorname{erf} c\left(\frac{y\sqrt{\mathrm{Sc}}}{2\sqrt{t}} + \sqrt{a_5 t}\right) \\
&\quad - \frac{a_6}{2a_5} e^{a_5 t - y\sqrt{a_5 \mathrm{Sc}}} \operatorname{erf} c\left(\frac{y\sqrt{\mathrm{Sc}}}{2\sqrt{t}} - \sqrt{a_5 t}\right) \\
&\quad - \frac{1}{\sqrt{\pi}} \int_0^t \frac{f(t-s) e^{-H_1 s - y^2/4s}}{\sqrt{s}} ds, \\
T(y,t) &= \operatorname{erf} c\left(\frac{y\sqrt{\Pr}}{2\sqrt{t}}\right), \\
\frac{\partial T(0,t)}{\partial y} &= -\frac{\sqrt{\Pr}}{\sqrt{\pi t}}.
\end{aligned}
\tag{40}
$$

5.3. Solutions in the Absence of Free Convection. Let us assume that the flow is caused only due to bounding plate and the corresponding buoyancy forces are zero equivalently it shows the absence of free convection due to the differences in temperature and mass gradients that is, the terms Gr and Gm are zero. This shows that the convective parts of velocities are zero in both cases of ramped wall and constant temperature and the flow is only governed by the mechanical part of velocities given by (29) and (36).

5.4. Solutions in the Absence of Mechanical Effects. In this case we assume that the infinite plate is in static position at every time; that is, the function $f(t)$ is zero for all values of t and the mechanical parts for both ramped and constant wall temperature are equivalently zero. In such a situation, the motion in the fluid is induced only due to the free convection. Therefore, the velocities of the fluid in both cases of ramped and constant wall temperature are only represented by their convective parts given by (28) and (36).

5.5. Solution in the Absence of Magnetic Parameter ($M \to 0$). It is clear from (20) and (24) that the temperature and concentration distributions are not influenced by the magnetic parameter M, and the velocities with $M = 0$ for both ramped and constant wall temperature are given by

$$
\begin{aligned}
u(y,t) &= a_1 \int_0^t \left(\frac{e^{a_{10}(t-s)} \operatorname{erf}\left(\sqrt{a_{10}(t-s)}\right)}{(a_{10})^{3/2}} - \frac{2\sqrt{t-s}}{\sqrt{\pi} a_{10}}\right) \\
&\quad \times \frac{e^{-K_p s - y^2/4s}}{\sqrt{\pi s}} ds \\
&\quad + \left[\frac{a_1}{\pi a_{10}} \int_0^{t-1} \frac{2\sqrt{t-1-s} e^{-K_p s - y^2/4s}}{\sqrt{s}} ds\right] H(t-1)
\end{aligned}
$$

$$
\begin{aligned}
&- \left[\frac{a_1}{(a_{10})^{3/2}\sqrt{\pi}} \int_0^{t-1} \left(\left(\operatorname{erf}\left(\sqrt{a_{10}(t-1-s)} \right) \right. \right. \right. \\
&\qquad \left. \left. \left. \times e^{a_{10}(t-1-s)-K_p s-y^2/4s} \right) \right. \right. \\
&\qquad \left. \left. \times \left(\sqrt{s}\right)^{-1} \right) ds \right] \\
&\times H(t-1) \\
&+ a_4 \int_0^t \left(\frac{e^{a_{11}(t-s)} \operatorname{erf}\left(\sqrt{a_{11}(t-s)} \right)}{\sqrt{a_{11}}} - \frac{2\sqrt{t-s}}{\sqrt{\pi} a_{10}} \right) \\
&\qquad \times \frac{e^{-K_p s-y^2/4s}}{\sqrt{\pi s}} ds \\
&+ \frac{a_3}{a_{10}} \left(t + \frac{\mathrm{Pr}_{\mathrm{eff}} y^2}{2} \right) \operatorname{erf} c\left(\frac{y\sqrt{\mathrm{Pr}_{\mathrm{eff}}}}{2\sqrt{t}} \right) \\
&- \frac{a_3}{a_{10}} \frac{y\sqrt{\mathrm{Pr}_{\mathrm{eff}}}\sqrt{t}}{\sqrt{\pi}} e^{-y^2 \mathrm{Pr}_{\mathrm{eff}}/4t} + \frac{a_3}{a_{10}^2} \operatorname{erf} c\left(\frac{y\sqrt{\mathrm{Pr}_{\mathrm{eff}}}}{2\sqrt{t}} \right) \\
&- \frac{1}{\sqrt{\pi}} \int_0^t \frac{f(t-s)\, e^{-K_p s-y^2/4s}}{\sqrt{s}} ds \\
&- \frac{a_3 e^{a_{10}t+y\sqrt{\mathrm{Pr}_{\mathrm{eff}} a_{10}}}}{2a_{10}^2} \operatorname{erf} c\left(\frac{y\sqrt{\mathrm{Pr}_{\mathrm{eff}}}}{2\sqrt{t}} + \sqrt{a_{10}t} \right) \\
&- \frac{a_3 e^{a_{10}t-y\sqrt{\mathrm{Pr}_{\mathrm{eff}} a_{10}}}}{2a_{10}^2} \operatorname{erf} c\left(\frac{y\sqrt{\mathrm{Pr}_{\mathrm{eff}}}}{2\sqrt{t}} - \sqrt{a_{10}t} \right) \\
&- \frac{a_3}{a_{10}} \left((t-1) + \frac{\mathrm{Pr}_{\mathrm{eff}} y^2}{2} \right) \operatorname{erf} c\left(\frac{y\sqrt{\mathrm{Pr}_{\mathrm{eff}}}}{2\sqrt{t-1}} \right) \\
&\times H(t-1) \\
&+ \frac{a_3}{a_{10}} \frac{y\sqrt{\mathrm{Pr}_{\mathrm{eff}}}\sqrt{t-1}}{\sqrt{\pi}} e^{-y^2 \mathrm{Pr}_{\mathrm{eff}}/4(t-1)} H(t-1) \\
&- \frac{a_6 e^{a_{11}t-y\sqrt{a_{11}\mathrm{Sc}}}}{2a_{11}} \operatorname{erf} c\left(\frac{y\sqrt{\mathrm{Sc}}}{2\sqrt{t}} - \sqrt{a_{11}t} \right) \\
&- \frac{a_3}{a_{10}^2} \operatorname{erf} c\left(\frac{y\sqrt{\mathrm{Pr}_{\mathrm{eff}}}}{2\sqrt{t-1}} \right) H(t-1) + \frac{a_6}{a_{11}} \operatorname{erf} c\left(\frac{y\sqrt{\mathrm{Sc}}}{2\sqrt{t}} \right) \\
&+ \frac{a_3 e^{a_{10}(t-1)+y\sqrt{\mathrm{Pr}_{\mathrm{eff}} a_{10}}}}{2a_{10}^2} \operatorname{erf} c\left(\frac{y\sqrt{\mathrm{Pr}_{\mathrm{eff}}}}{2\sqrt{t-1}} + \sqrt{a_{10}(t-1)} \right) \\
&\times H(t-1) \\
&+ \frac{a_3 e^{a_{10}(t-1)-y\sqrt{\mathrm{Pr}_{\mathrm{eff}} a_{10}}}}{2a_{10}^2} \operatorname{erf} c\left(\frac{y\sqrt{\mathrm{Pr}_{\mathrm{eff}}}}{2\sqrt{t-1}} - \sqrt{a_{10}(t-1)} \right) \\
&\times H(t-1) \\
&- \frac{a_6 e^{a_{11}t+y\sqrt{a_{11}\mathrm{Sc}}}}{2a_{11}} \operatorname{erf} c\left(\frac{y\sqrt{\mathrm{Sc}}}{2\sqrt{t}} + \sqrt{a_{11}t} \right),
\end{aligned}
$$

$$
\begin{aligned}
u(y,t) &= \frac{a_1}{\sqrt{\pi a_{10}}} \int_0^t \frac{e^{a_{10}(t-s)-K_p s-y^2/4s} \operatorname{erf}\left(\sqrt{a_{10}(t-s)} \right)}{\sqrt{s}} ds \\
&+ \frac{a_4}{\sqrt{\pi a_{11}}} \int_0^t \frac{e^{a_{11}(t-s)-K_p s-y^2/4s} \operatorname{erf}\left(\sqrt{a_{11}(t-s)} \right)}{\sqrt{s}} ds \\
&- \frac{a_3}{2a_{10}} e^{a_{10}t+y\sqrt{a_{10}\mathrm{Pr}_{\mathrm{eff}}}} \operatorname{erf} c\left(\frac{y\sqrt{\mathrm{Pr}_{\mathrm{eff}}}}{2\sqrt{t}} + \sqrt{a_{10}t} \right) \\
&- \frac{a_3}{2a_{10}} e^{a_{10}t-y\sqrt{a_{10}\mathrm{Pr}_{\mathrm{eff}}}} \operatorname{erf} c\left(\frac{y\sqrt{\mathrm{Pr}_{\mathrm{eff}}}}{2\sqrt{t}} - \sqrt{a_{10}t} \right) \\
&+ \frac{a_3}{a_{10}} \operatorname{erf} c\left(\frac{y\sqrt{\mathrm{Pr}_{\mathrm{eff}}}}{2\sqrt{t}} \right) + \frac{a_6}{a_{11}} \operatorname{erf} c\left(\frac{y\sqrt{\mathrm{Sc}}}{2\sqrt{t}} \right) \\
&- \frac{a_6}{2a_{11}} e^{a_{11}t+y\sqrt{a_{11}\mathrm{Sc}}} \operatorname{erf} c\left(\frac{y\sqrt{\mathrm{Sc}}}{2\sqrt{t}} + \sqrt{a_{11}t} \right) \\
&- \frac{1}{\sqrt{\pi}} \int_0^t \frac{f(t-s)\, e^{-K_p s-y^2/4s}}{\sqrt{s}} ds \\
&- \frac{a_6}{2a_{11}} e^{a_{11}t-y\sqrt{a_{11}\mathrm{Sc}}} \operatorname{erf} c\left(\frac{y\sqrt{\mathrm{Sc}}}{2\sqrt{t}} - \sqrt{a_{11}t} \right).
\end{aligned} \tag{41}
$$

6. Special Cases

We noted that the solutions for velocity obtained in Section 3 are more general. Therefore, we want to discuss some special cases of the present solutions together with some limiting solutions in order to know more about the physical insight of the problem. Hence, we discuss the following important special cases in the case of ramped wall temperature whose technical relevance is well known in the literature. Similarly we can discuss some special cases of constant wall temperature solutions.

6.1. Case-I: $f(t) = fH(t)$. In this first case we take the arbitrary function $f(t) = fH(t)$, where $f(\cdot)$ is a dimensionless constant and $H(\cdot)$ denotes the unit step function. After time $t = 0$, the infinite inclined plate applies a constant shear stress to the fluid. The convective part of the velocity remains unchanged while the mechanical part takes the following form:

$$
u_m(y,t) = -\frac{f}{\sqrt{\pi}} \int_0^t \frac{e^{-y^2/4s-H_1 s}}{\sqrt{s}} ds, \tag{42}
$$

equivalently

$$
u_m(y,t) = -\frac{f}{\sqrt{H_1}} e^{-y\sqrt{H_1}} + \frac{2f}{\sqrt{\pi}} \int_{\sqrt{t}}^{\infty} e^{-y^2/4z^2-H_1 z^2} dz, \tag{43}
$$

for $K_p \neq 0$, $M \neq 0$. Moreover, if we take $M = 0$, (42) reduces to the form

$$
u_m(y,t) = -\frac{f}{\sqrt{K_p}} e^{-y\sqrt{K_p}} + \frac{2f}{\sqrt{\pi}} \int_{\sqrt{t}}^{\infty} e^{-y^2/4z^2-K_p z^2} dz, \tag{44}
$$

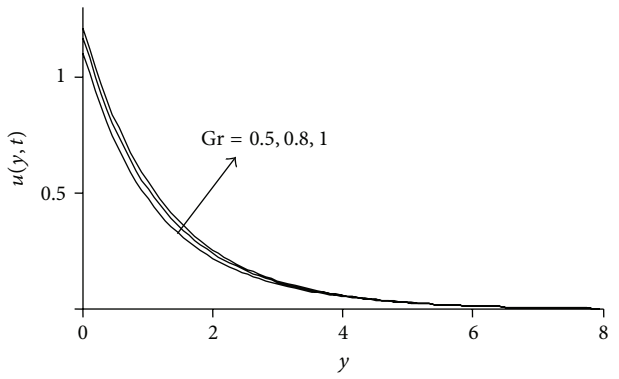

Figure 2: Velocity profiles for $\mathrm{Pr}_{\mathrm{eff}} = 0.350$ ($N_r = 1$, Pr = 0.7), $K_p = 0.7$, $t = 1.2$ and different values of Gr when the plate applies a constant shear stress $f = -1$.

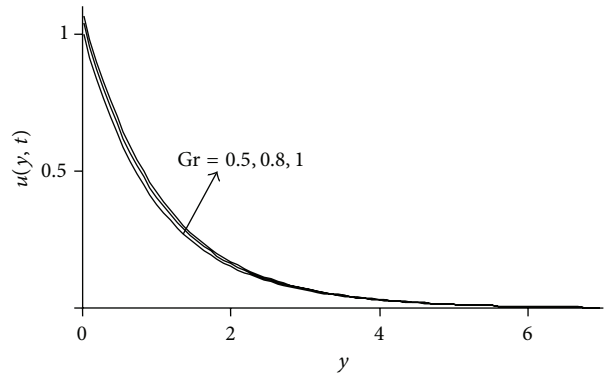

Figure 3: Velocity profiles for $\mathrm{Pr}_{\mathrm{eff}} = 0.350$ ($N_r = 1$, Pr = 0.7), $K_p = 0.7$, $t = 0.9$ and different values of Gr when the plate applies a constant shear stress $f = -1$.

which is equivalent to [28, Equation (28)] with the correction of $\sqrt{K_p}$.

Furthermore, in the absence of both $K_p = 0$ and $M = 0$, (42) is identical with [23, Equation (23)]

$$u_m(y,t) = -\frac{f}{\sqrt{\pi}} \int_0^t \frac{e^{-y^2/4s}}{\sqrt{s}} ds. \tag{45}$$

6.2. Case-II: $f(t) = f\sin(\omega t)$. In the second case, we take the arbitrary function of the form $f(t) = f\sin(\omega t)$ in which the plate applies an oscillating shear stress to the fluid. Here ω denotes the dimensionless frequency of the shear stress. As previously, the convective part of velocity remains the same whereas the mechanical part takes the form

$$u_m(y,t) = -\frac{f}{\sqrt{\pi}} \int_0^t \frac{\sin(\omega t - \omega s)\, e^{-y^2/4s - H_1 s}}{\sqrt{s}} ds. \tag{46}$$

It can be further written as a sum of the steady-state and transient solutions

$$u_m(y,t) = u_{ms}(y,t) + u_{mt}(y,t), \tag{47}$$

where

$$\begin{aligned} u_{ms}(y,t) &= -\frac{f}{\sqrt{\pi}} \int_0^t \frac{\sin(\omega t - \omega s)\, e^{-y^2/4s - H_1 s}}{\sqrt{s}} ds, \\ u_{mt}(y,t) &= \frac{f}{\sqrt{\pi}} \int_t^\infty \frac{\sin(\omega t - \omega s)\, e^{-y^2/4s - H_1 s}}{\sqrt{s}} ds. \end{aligned} \tag{48}$$

By taking $M = 0$, the steady-state component reduces to [28, Equation (35)]

$$u_{ms}(y,t) = -\frac{f}{\sqrt{\pi}} \int_0^t \frac{\sin(\omega t - \omega s)\, e^{-y^2/4s - K_p s}}{\sqrt{s}} ds. \tag{49}$$

In addition when $K_p = 0$, physically it corresponds to the absence of porous effects and (49) results in

$$u_{ms}(y,t) = -\frac{f}{\sqrt{\pi}} \int_0^t \frac{\sin(\omega t - \omega s)\, e^{-y^2/4s}}{\sqrt{s}} ds, \tag{50}$$

which can be written in simplified form as

$$u_{ms}(y,t) = \frac{f}{\sqrt{\omega}} \exp\left(-y\sqrt{\frac{\omega}{2}}\right) \cos\left(\omega t - y\sqrt{\frac{\omega}{2}} + \frac{\pi}{4}\right), \tag{51}$$

equivalent to [23, Equation (33)].

6.3. Case-III: $f(t) = ft^a$ ($a > 0$). In the final case, we take $f(t) = ft^a$, in which the plate applies an accelerating shear stress to the fluid where the mechanical part takes the following form:

$$u_m(y,t) = -\frac{f}{\sqrt{\pi}} \int_0^t \frac{(t-s)^a e^{-y^2/4s - H_1 s}}{\sqrt{s}} ds. \tag{52}$$

The corresponding solution for $M = 0$, namely,

$$u_m(y,t) = -\frac{f}{\sqrt{\pi}} \int_0^t \frac{(t-s)^a e^{-y^2/4s - K_p s}}{\sqrt{s}} ds, \tag{53}$$

is identical with [28, Equation (32)].

Additionally, if we take $K_p = 0$, (53) yields

$$u_m(y,t) = -\frac{f}{\sqrt{\pi}} \int_0^t \frac{(t-s)^a e^{-y^2/4s}}{\sqrt{s}} ds. \tag{54}$$

7. Results and Discussion

In order to understand the physical aspects of the problem, the numerical results for velocity, temperature, and concentration are computed and plotted for various parameters of interest such as magnetic parameter M, porosity parameter K_p, effective Prandtl number $\mathrm{Pr}_{\mathrm{eff}}$, Grashof number Gr, modified Grashof number Gm, dimensionless time t, Schmidt number Sc, and shear stress f. The graphs for velocity are shown in Figures 2–17, where $t = 1.2$ corresponds to isothermal velocity and $t = 0.9$ is for ramped velocity. Figures 18–21 are plotted to show the temperature variations for two types of boundary conditions, namely, ramped and constant wall temperatures. Furthermore, Figure 22 is displayed to show

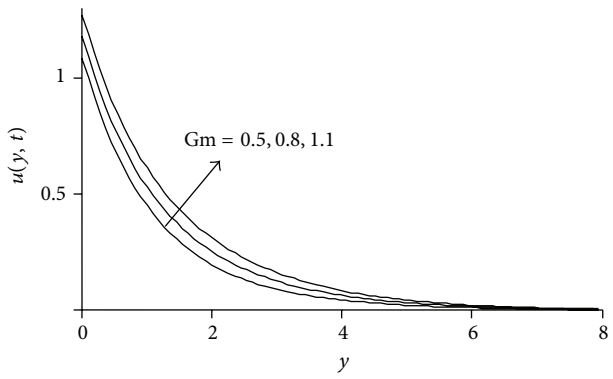

Figure 4: Velocity profiles for $\mathrm{Pr}_{\mathrm{eff}} = 0.350$ ($N_r = 1$, Pr = 0.7), $K_p = 0.7$, $t = 1.2$ and different values of Gm when the plate applies a constant shear stress $f = -1$.

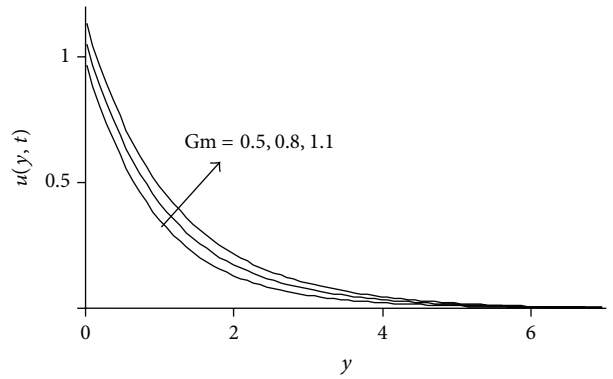

Figure 5: Velocity profiles for $\mathrm{Pr}_{\mathrm{eff}} = 0.350$ ($N_r = 1$, Pr = 0.7), $K_p = 0.7$, and $t = 0.9$ and different values of Gm when the plate applies a constant shear stress $f = -1$.

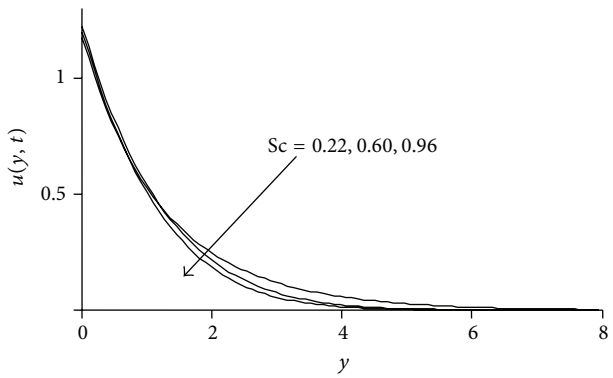

Figure 6: Velocity profiles for $\mathrm{Pr}_{\mathrm{eff}} = 0.350$ ($N_r = 1$, Pr = 0.7), $K_p = 0.7$, and $t = 1.2$ and different values of Sc when the plate applies a constant shear stress $f = -1$.

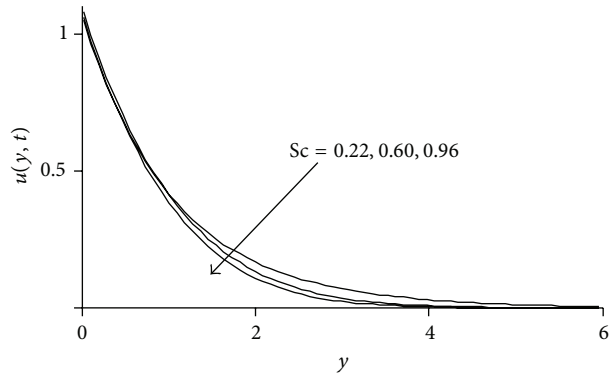

Figure 7: Velocity profiles for $\mathrm{Pr}_{\mathrm{eff}} = 0.350$ ($N_r = 1$, Pr = 0.7), $K_p = 0.7$, and $t = 0.9$ and different values of Sc when the plate applies a constant shear stress $f = -1$.

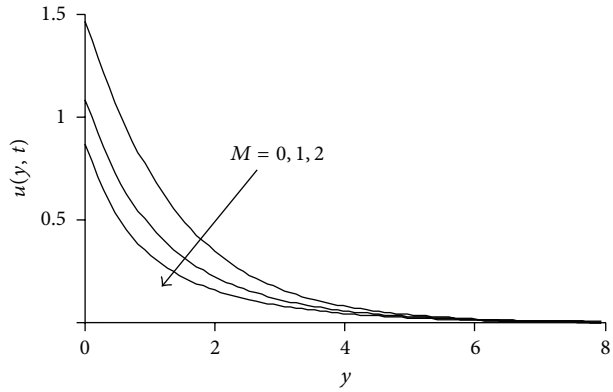

Figure 8: Velocity profiles for $\mathrm{Pr}_{\mathrm{eff}} = 0.350$ ($N_r = 1$, Pr = 0.7), $K_p = 0.7$, and $t = 1.2$ and different values of M when the plate applies a constant shear stress $f = -1$.

variations in fluid concentration. Figures 2 and 3 illustrate the influence of Grashof number Gr on the velocity. It is observed that velocity increases with increasing Gr. This implies that thermal buoyancy force tends to accelerate velocity for both ramped temperature and isothermal plates. In Figures 4 and 5, the velocity profiles for different values modified Grashof number Gm are shown. It is found that velocity increases on increasing Gm for both ramped temperature and isothermal plate. Further, it can be observed that the velocity and boundary layer thickness decrease along y with increasing distance from the leading edge. Moreover, from Figures 4 and 5, we observed that the amplitude of velocity in case of isothermal plate is greater and converges slowly as compared to ramped velocity. In Figures 6 and 7, the velocity profiles are shown for different values of Schmidt number Sc. Here the values of Sc are chosen 0.22, 0.60, and 0.96. to represent the presence of species by hydrogen, water vapor, and carbon dioxide respectively. It is observed that the velocity decreases with increasing Schmidt number. Physically, this refers to the phenomenon that increasing Schmidt number implies the dominance of the viscous forces over the diffusional effects. As a result, the flow will be therefore decelerated with a rise in Schmidt number. The velocity profiles for different values of magnetic parameter M are shown in Figures 8 and 9. The range of magnetic field is taken from 0 to 2. It is found that the velocity is decreasing with increasing values of M in both cases of ramped and isothermal plates. Physically, it is true due to the fact that increasing values of M causes the frictional force to increase which tends to resist the fluid flow, thus reducing its velocity. It is further observed that when

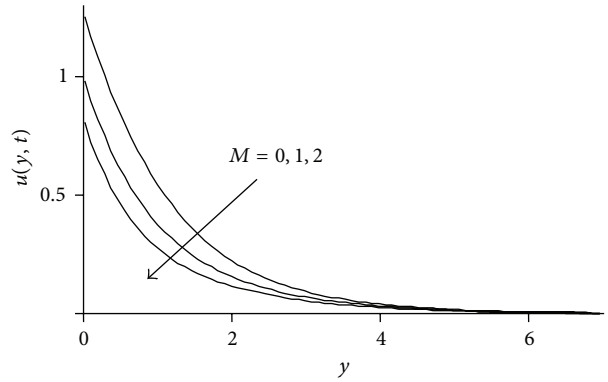

Figure 9: Velocity profiles for $\mathrm{Pr}_{\mathrm{eff}} = 0.350$ ($N_r = 1$, Pr = 0.7), $K_p = 0.7$, and $t = 0.9$ and different values of M when the plate applies a constant shear stress $f = -1$.

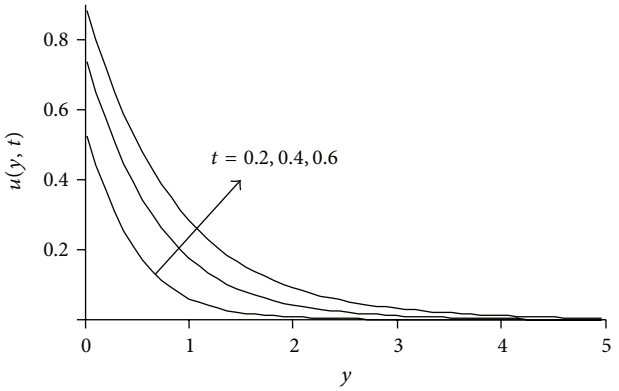

Figure 10: Velocity profiles for $\mathrm{Pr}_{\mathrm{eff}} = 0.350$ ($N_r = 1$, Pr = 0.7) and $K_p = 0.7$ and different values of t when the plate applies a constant shear stress $f = -1$.

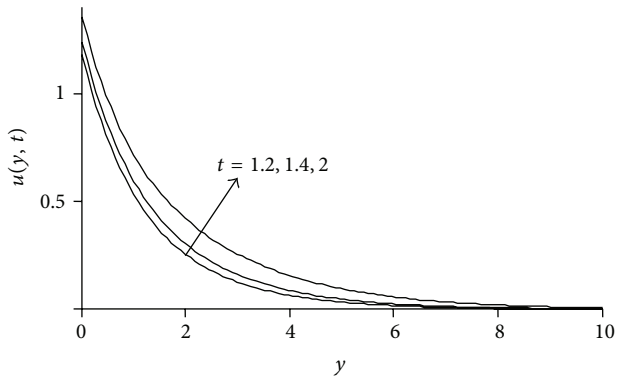

Figure 11: Velocity profiles for $\mathrm{Pr}_{\mathrm{eff}} = 0.350$ ($N_r = 1$, Pr = 0.7) and $K_p = 0.7$ and different values of t when the plate applies a constant shear stress $f = -1$.

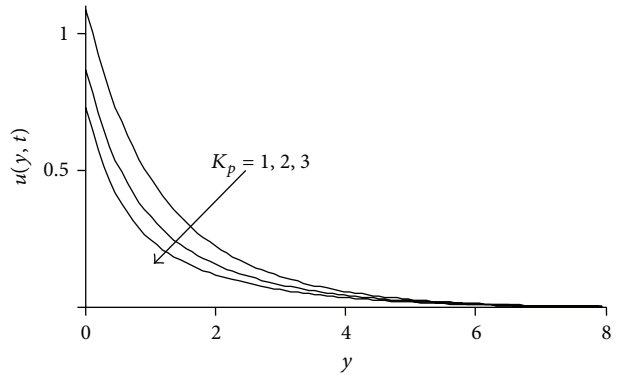

Figure 12: Velocity profiles for $\mathrm{Pr}_{\mathrm{eff}} = 0.350$ ($N_r = 1$, Pr = 0.7) and $t = 1.2$ and different values of K_p when the plate applies a constant shear stress $f = -1$.

the magnetic field imposed on the flow is zero ($M = 0$), the MHD effect vanishes and the flow is termed as hydrodynamic flow. Physically, it is true due to the fact that increasing values of M causes the frictional force to increase which tends to resist the fluid flow, thus reducing its velocity. Figures 10 and 11 are plotted to see the difference between the ramped and isothermal plate velocities. The values of $t < 1$ correspond to ramp velocity whereas $t > 1$ is for isothermal plate. It is found that ramp velocity is less than isothermal plate and converges faster. Further velocity in both cases increases with increasing time. The effects of inverse permeability parameter K_p on the velocity profiles are presented in Figures 12 and 13. It is found that velocity decreases with increasing K_p in both cases of ramp and isothermal plate. Physically, it is due to the fact that increasing permeability of the porous medium increases the resistance and consequently velocity decreases. This observation is an excellent agreement with the previous study [28, Figure 3]. The effects of the shear stress f induced by the bounding plate on the nondimensional velocity profiles are shown in Figures 14 and 15. The velocity of fluid is found to decrease with increasing f in both cases of ramped velocity and isothermal plate. Graphical results to show the influence of the effective Prandtl number $\mathrm{Pr}_{\mathrm{eff}}$ on velocity profiles are presented in Figures 16 and 17. It is observed that the velocity is a decreasing function with respect to $\mathrm{Pr}_{\mathrm{eff}}$. These graphical results are in accordance with [28, Figure 2]. The temperature variations against y for various values of effective Prandtl number are highlighted in Figures 18 and 19. The significant decrease of the temperature is found as a result of an increase of the effective Prandtl number. The fluid temperature decreases from maximum at the boundary to a minimum value as far from the plate in both cases of ramped and constant temperature. In Figures 20 and 21, we have shown the temperature variations for two types of boundary conditions ramped and constant plate temperatures. It is noted that the fluid temperature is greater in the case of isothermal plate than in the case of ramped temperature at the plate. This should be expected since, in the latter case, the heating of the fluid takes place more gradually than in the isothermal case [29]. Moreover, with increasing time, the temperature is found to increase in both cases of ramped and constant wall temperature. The concentration profiles for different values of Schmidt number Sc are shown in Figure 22. It is clear from this figure that the concentration profiles and the concentration boundary layer

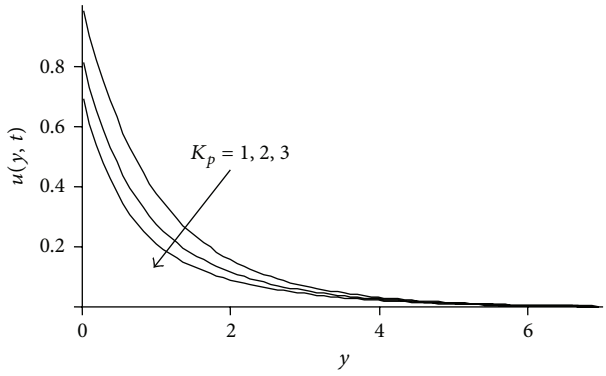

FIGURE 13: Velocity profiles for $\mathrm{Pr}_{\mathrm{eff}} = 0.350$ ($N_r = 1$, Pr = 0.7) and $t = 0.9$ and different values of K_p when the plate applies a constant shear stress $f = -1$.

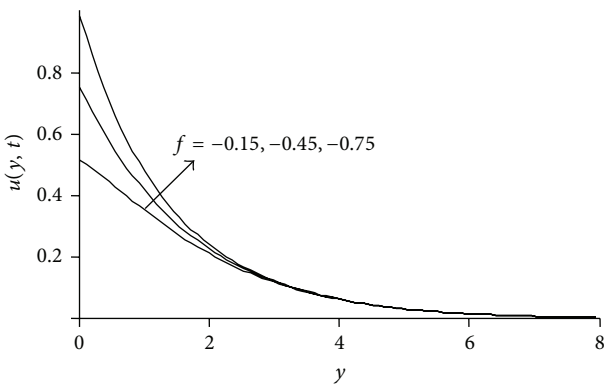

FIGURE 14: Velocity profiles for $\mathrm{Pr}_{\mathrm{eff}} = 0.350$ ($N_r = 1$, Pr = 0.7), $K_p = 0.7$, and $t = 1.2$ and different values of constant shear stress f.

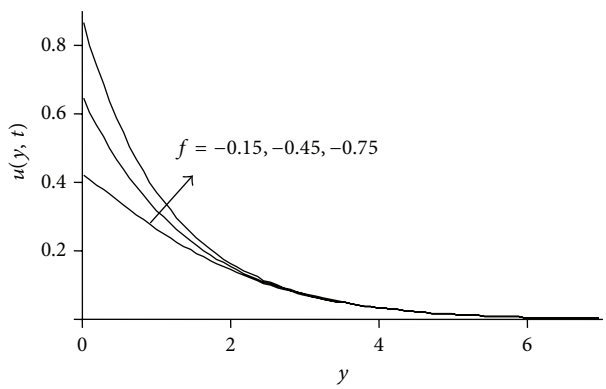

FIGURE 15: Velocity profiles for $\mathrm{Pr}_{\mathrm{eff}} = 0.350$ ($N_r = 1$, Pr = 0.7), $K_p = 0.7$, and $t = 0.9$ and different values of constant shear stress f.

thickness decrease with increasing values of Sc. Physically, it is true, since increase of Sc means decrease of molecular diffusivity which results in a decrease of concentration boundary layer.

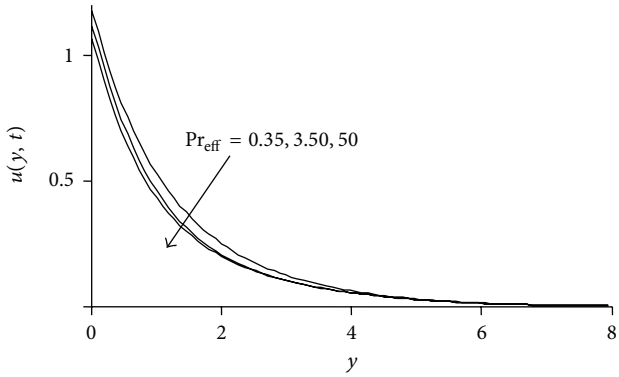

FIGURE 16: Velocity profiles for $K_p = 0.7$ and $t = 1.2$ and different values of $\mathrm{Pr}_{\mathrm{eff}}$ when the plate applies a constant shear stress $f = -1$.

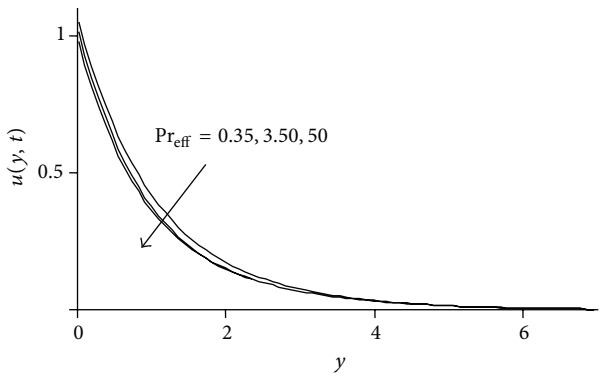

FIGURE 17: Velocity profiles for $K_p = 0.7$ and $t = 0.9$ and different values of $\mathrm{Pr}_{\mathrm{eff}}$ when the plate applies a constant shear stress $f = -1$.

8. Conclusions

The purpose of this work was to analyze the unsteady MHD free convection flow of an incompressible viscous fluid over an infinite inclined plate with ramped wall temperature and applies an arbitrary shear stress to the fluid. Exact solutions for velocity, temperature (for both cases of ramped and constant wall temperature), and concentration are obtained using the Laplace transform technique and expressed in terms of the complementary error function. They satisfy all imposed initial and boundary conditions. These solutions are plotted in various figures for different parameters of interest. The following conclusions are extracted from this study.

(i) The velocity of the fluid $u(y, t)$ can be written as a sum of its convective and thermal components.

(ii) For the velocity solution in which the plate applies an oscillating shear stress to the fluid $f(t) = f \sin(\omega t)$, the mechanical part can be further written as a sum of the steady-state and transient solutions.

(iii) The concentration boundary layer thickness decreases with increasing values of Sc.

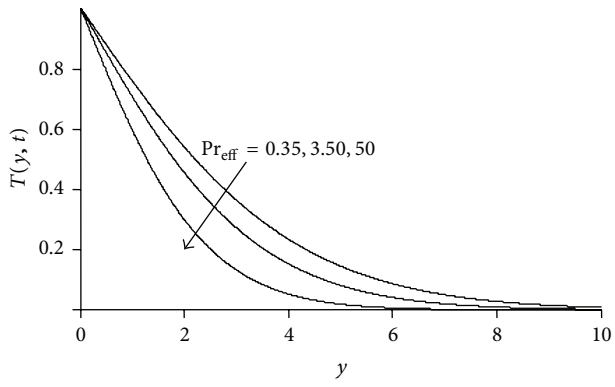

FIGURE 18: Temperature profile for $t = 1.2$ and different values of $\mathrm{Pr}_{\mathrm{eff}}$.

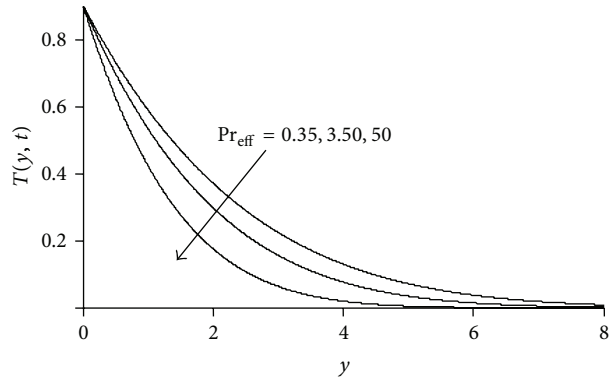

FIGURE 19: Temperature profile for $t = 0.9$ and different values of $\mathrm{Pr}_{\mathrm{eff}}$.

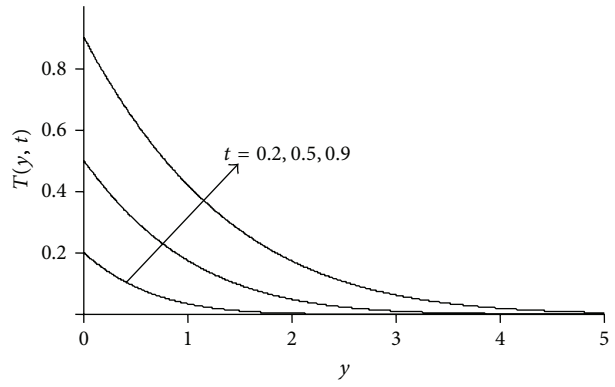

FIGURE 20: Temperature profiles for $\mathrm{Pr}_{\mathrm{eff}} = 0.350$ ($N_r = 1$, $\mathrm{Pr} = 0.7$) and different values of t.

(iv) The thermal boundary layer thickness in case of ramped wall temperature is less than isothermal wall temperature.

(v) The magnetic parameter M develops shear resistance which retards the fluid whereas the inverse permeability parameter K_p enhances the fluid motion.

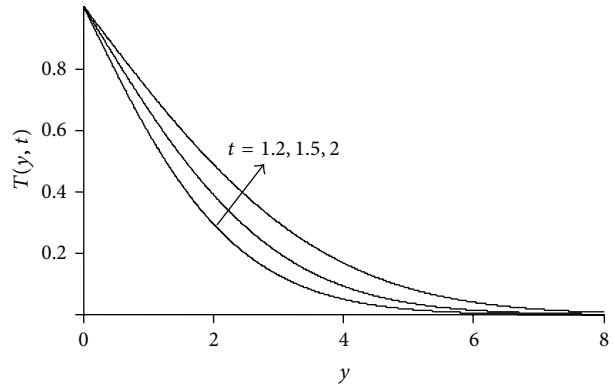

FIGURE 21: Temperature profiles for $\mathrm{Pr}_{\mathrm{eff}} = 0.350$ ($N_r = 1$, $\mathrm{Pr} = 0.7$) and different values of t.

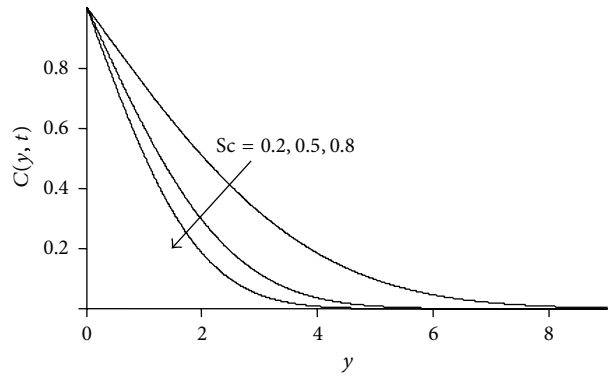

FIGURE 22: Concentration profiles for $t = 1.2$ and different values of Sc.

Conflict of Interests

The authors declare that there is no conflict of interests regarding the publication of this paper.

Acknowledgment

The authors would like to acknowledge MOE and Research Management Centre—UTM for the financial support through vote numbers 04H27, and 4F255 for this research.

References

[1] B. Rich, "An investigation of heat transfer from an inclined flat plate in free convection," *Transactions of the ASME*, vol. 75, pp. 489–499, 1953.

[2] K. Stewartson, "On the free convection from a horizontal plate," *Zeitschrift für Angewandte Mathematik und Physik*, vol. 9, no. 3, pp. 276–282, 1958.

[3] W.-S. Yu and H.-T. Lin, "Free convection heat transfer from an isothermal plate with arbitrary inclination," *Wärme- und Stoffübertragung*, vol. 23, no. 4, pp. 203–211, 1988.

[4] T. S. Chen, H. C. Tien, and B. F. Armaly, "Natural convection on horizontal, inclined, and vertical plates with variable surface temperature or heat flux," *International Journal of Heat and Mass Transfer*, vol. 29, no. 10, pp. 1465–1478, 1986.

[5] P. Ganesan and K. Ekambavanan, "Finite difference solution of unsteady natural convection boundary layer flow over an inclined plate with variable surface temperature," *Wärme- und Stoffübertragung*, vol. 30, no. 2, pp. 63–69, 1994.

[6] N. Onur and M. K. Aktaş, "An experimental study on the effect of opposing wall on natural convection along an inclined hot plate facing downward," *International Communications in Heat and Mass Transfer*, vol. 25, no. 3, pp. 389–397, 1998.

[7] H. S. Takhar, A. J. Chamkha, and G. Nath, "Effects of non-uniform wall temperature or mass transfer in finite sections of an inclined plate on the MHD natural convection flow in a temperature stratified high-porosity medium," *International Journal of Thermal Sciences*, vol. 42, no. 9, pp. 829–836, 2003.

[8] P. Ganesan and G. Palani, "Finite difference analysis of unsteady natural convection MHD flow past an inclined plate with variable surface heat and mass flux," *International Journal of Heat and Mass Transfer*, vol. 47, no. 19-20, pp. 4449–4457, 2004.

[9] G. Palani, *Convection Effects on Flow Past an Inclined Plate with Variable Surface Tem- Peratures in Water at 40c*, 2008.

[10] S. Siddiqa, S. Asghar, and M. A. Hossain, "Natural convection flow over an inclined flat plate with internal heat generation and variable viscosity," *Mathematical and Computer Modelling*, vol. 52, no. 9-10, pp. 1739–1751, 2010.

[11] A. Begum, M. A. Maleque, M. Ferdows, and M. Ota, "Pressure effects on unsteady free convection and heat transfer flow of an incompressible fluid past a semi-infinite inclined plate with impulsive and uniformly accelerated motion," *Applied Mathematical Sciences*, vol. 6, no. 68, pp. 3347–3365, 2012.

[12] S. Masthanrao, K. Balamurugan, and S. Varma, "Chemical reaction effects on mhd free convection flow through a porous medium bounded by an inclined surface," *International Journal of Mathematics*, vol. 3, no. 3, pp. 13–22, 2013.

[13] R. K. Tripathi and A. Sau, "Combined heat and mass transfer in natural convection on horizontal and inclined plates with variable surface temperature/concentration or heat/mass flux," *Acta Mechanica*, vol. 109, no. 1–4, pp. 227–235, 1995.

[14] M. S. Alam, M. M. Rahman, and M. A. Sattar, "MHD free convective heat and mass transfer flow past an inclined surface with heat generation," *Thammasat International Journal of Science and Technology*, vol. 11, no. 4, pp. 1–8, 2006.

[15] M. S. Alam, M. M. Rahman, and M. A. Sattar, "Effects of variable suction and thermophoresis on steady MHD combined free-forced convective heat and mass transfer flow over a semi-infinite permeable inclined plate in the presence of thermal radiation," *International Journal of Thermal Sciences*, vol. 47, no. 6, pp. 758–765, 2008.

[16] M. Bhuvaneswari, S. Sivasankaran, and M. Ferdows, "Lie group analysis of natural convection heat and mass transfer in an inclined surface with chemical reaction," *Nonlinear Analysis: Hybrid Systems*, vol. 3, no. 4, pp. 536–542, 2009.

[17] F. Ali, I. Khan, S. Shafie et al., "Conjugate effects of heat and mass transfer on mhd free convection flow over an inclined plate embedded in a porous medium," *PloS One*, vol. 8, no. 6, article e65223, 2013.

[18] O. D. Makinde, "Thermodynamic second law analysis for a gravity-driven variable viscosity liquid film along an inclined heated plate with convective cooling," *Journal of Mechanical Science and Technology*, vol. 24, no. 4, pp. 899–908, 2010.

[19] O. D. Makinde, "Second law analysis for variable viscosity hydromagnetic boundary layer flow with thermal radiation and Newtonian heating," *Entropy*, vol. 13, no. 8, pp. 1446–1464, 2011.

[20] S. C. Saha, C. Lei, and J. C. Patterson, "On the natural convection boundary layer adjacent to an inclined flat plate subject to ramp heating," in *Proceedings of the 16th Australasian Fluid Mechanics Conference (AFMC '07)*, pp. 121–124, School of Engineering, The University of Queensland, December 2007.

[21] S. C. Saha, J. C. Patterson, and C. Lei, "Scaling of natural convection of an inclined flat plate: ramp cooling condition," *International Journal of Heat and Mass Transfer*, vol. 53, no. 23-24, pp. 5156–5166, 2010.

[22] Z. Ismail, A. I. Ilyas Khan, A. Hussanan, and S. Shafie, "Mhd double diffusion flow by free convection past an infinite inclined plate with ramped wall temperature in a porous medium," *Malaysian Journal of Fundamental and Applied Sciences*, vol. 9, no. 5, 2013.

[23] C. Fetecau, C. Fetecau, and M. Rana, "General solutions for the unsteady flow of second-grade fluids over an infinite plate that applies arbitrary shear to the fluid," *Zeitschrift fur Naturforschung Section A-J*, vol. 66, pp. 753–759, 2011.

[24] E. Magyari and A. Pantokratoras, "Note on the effect of thermal radiation in the linearized Rosseland approximation on the heat transfer characteristics of various boundary layer flows," *International Communications in Heat and Mass Transfer*, vol. 38, no. 5, pp. 554–556, 2011.

[25] M. Narahari and B. K. Dutta, "Effects of thermal radiation and mass diffusion on free convection flow near a vertical plate with newtonian heating," *Chemical Engineering Communications*, vol. 199, no. 5, pp. 628–643, 2012.

[26] S. K. Ghosh and O. A. Beg, "Theoretical analysis of radiative effects on transient free convection heat transfer past a hot vertical surface in porous media," *Nonlinear Analysis: Modelling and Control*, vol. 13, pp. 419–432, 2008.

[27] A. David Maxim Gururaj and S. P. Anjali Devi, "MHD boundary layer flow with forced convection past a nonlinearly stretching surface with variable temperature and nonlinear radiation effects," *International Journal of Development Research*, vol. 4, pp. 075–080, 2014.

[28] C. Fetecau, M. Rana, and C. Fetecau, "Radiative and porous effects on free convection flow near a vertical plate that applies shear stress to the fluid," *Zeitschrift fur Naturforschung Section A-J*, vol. 68, pp. 130–138, 2013.

[29] P. Chandran, N. C. Sacheti, and A. K. Singh, "Natural convection near a vertical plate with ramped wall temperature," *Heat and Mass Transfer*, vol. 41, no. 5, pp. 459–464, 2005.